VERTAISARVIOITU
KOLLEGIALT GRANSKAD
PEER-REVIEWED
www.tsv.fi/tunnus

Fast boundary element simulation of noise emission from vibrating structures

Seppo Järvenpää, Tomi Huttunen, Antti Vanne, Matti Malinen, Janne Roivainen, and Pasi Ylä-Oijala[1]

Summary. A fast boundary element method (FBEM) based on multilevel fast multipole algorithm (MLFMA) is introduced for simulating acoustic emission from large vibrating structures. The vibration of a structure is first simulated using a finite element method (FEM). The surface velocity distribution, extracted from the FEM result, is then used a source term in FBEM. The fast acoustic BEM solver utilizes a special broadband version of MLFMA that allows efficient and accurate modeling of large scale acoustics problems on a broad range of frequencies.

Introduction

Vibration of machines can lead into decreased life time and undesired noise to surrounding environment. The capability of predicting acoustic field distribution generated by a vibrating structure with numerical simulations is thus of great importance in the designing of new machinery. With the help of the numerical simulations, it is possible to optimize the design so that vibration of the structure and noise emitted to the environment are minimized.

Assuming a weak coupling between the structure (a machine) and surrounding medium (air), the simulation work flow can be separated into two parts. First, the vibration of the structure is simulated using a finite element method (FEM). An abundance of FEM tools can be found for the mechanical modeling. Second, the surface velocity distribution is extracted from the FEM results and resulting acoustic emission can be computed using an acoustic simulation tool.

A linear wave equation forms an acceptable model for acoustic fields in many fluids, such as air and water. Using assumption of time-harmonic excitation, the wave equation reduces to Helmholtz equation in the frequency domain. FEM and the method of finite differences (FDM) are commonly used numerical approaches to find solutions for Helmholtz equation. In wave scattering and emission problems containing unbounded

---

[1]Corresponding author. `pasi.yla-oijala@aalto.fi`

domains the solution propagates into infinity requiring different solution strategies than in problems where the domain is bounded. The boundary element method (BEM) [1, 2] is an attractive option for that kind of problems, since the BEM solution automatically satisfies the necessary radiation conditions at infinity, and avoids the use of additional absorbing boundary conditions needed e.g., in FEM and FDM. Another great benefit of BEM is that it requires surfaces meshes only. This property, compared to methods requiring volumetric meshing, leads to a significant reduction on the number of degrees of freedom and essentially simplifies the mesh generation procedure and required data structures.

BEM takes into account all complex diffraction and multiple reflection phenomena and thus provides accurate full-wave solutions for complex wave scattering and emission problems. The main drawback of the traditional BEM based on direct linear system solvers, however, is its bad scaling with respect to the number of degrees of freedom. Both the time and memory needed to solve the problem increase very rapidly with respect to the employed number of degrees of freedom.

Using iterative, e.g., Krylov subspace, techniques it is possible to enlarge the size of the problems to be solved, but only up to a certain limit. As the size of the problem is large enough the solution of the linear system still requires so much computer resources that it is not doable even with the most powerful super-computing facilities. An answer to this challenge is provided by fast solution strategies. These methods are advanced techniques that significantly reduce the high computational load of BEM-based solvers and enable solutions of several orders of magnitude larger problems than is possible with standard solvers, iterative or direct. Recent advances in the fast multipole methods for acoustics problems are reviewed e.g., in [3] and [4].

We introduce a special version of the multilevel fast multipole algorithm (MLFMA). The employed version of MLFMA utilizes special translators [5] and interpolators [6, 7] that allow efficient and error controllable solutions of problems containing up to a few million of degrees of freedom in broad frequency range and arbitrary mesh density. The method is used to solve the matrix equation arising from BEM formulation of the mixed boundary value problem of Helmholtz equation based on the combined Helmholtz integral equation, known also as Burton-Miller equation [8]. This equation avoids spurious internal resonances and allows numerically efficient stabilization of the hyper-singular operator [9]. The original methodology introduced previously in [5, 9, 10] has been further enhanced in [6, 7, 11].

In this study, a fast BEM solver based on special broadband version of MLFMA is applied for simulating acoustic emission from vibrating structures. The surface velocity distribution, extracted from the FEM result, is used as a source for the acoustic solver. To efficiently model large vibrating structures also computation of the source term is accelerated with MLFMA. An electric motor is used as a model problem and comparisons with high-frequency approximation are made.

Acoustic modeling

We begin by introducing the acoustic wave problem and formulate it as a mixed boundary value problem of Helmholtz equation. Then the boundary element method (BEM) formulation is provided and it is demonstrated how the solution of the matrix equation can be accelerated with the multilevel fast multipole algorithm (MLFMA).

Reduced wave equation

Consider acoustic wave propagation in homogeneous isotropic medium with constant density ρ (e.g., in air 1.2041 kg/m^3) and speed of sound c (e.g., in air 340 m/s). Particle velocity $\boldsymbol{v}$ is obtained from velocity potential ϕ as

$$\boldsymbol{v} = \frac{1}{\rho}\nabla\phi. \tag{1}$$

In the linearized theory, potential ϕ satisfies wave equation

$$\frac{\partial^2\phi}{\partial t^2} - c^2\nabla \cdot \nabla\phi = 0 \tag{2}$$

in a source free medium. By assuming harmonic time-dependence, i.e., all functions are of the form

$$u'(\boldsymbol{r}, t) = u(\boldsymbol{r})\, e^{-i\omega t}, \tag{3}$$

where $\omega = 2\pi f$ is the angular frequency, f is the frequency, and t is time, wave equation (2) reduces to Helmholtz equation

$$\left(\nabla^2 + k^2\right)\phi = 0. \tag{4}$$

Here $k = \omega/c$ is the wavenumber and $\nabla^2 = \nabla \cdot \nabla$ denotes Laplacian operator. Pressure of an acoustic wave is the time derivative of ϕ

$$p = -\frac{\partial\phi}{\partial t} = i\omega\phi. \tag{5}$$

Hence, also the acoustic pressure satisfies homogeneous Helmholtz equation. On the surfaces the (specific) surface impedance is defined as the ratio of acoustic pressure and the normal velocity

$$Z = \frac{p}{\boldsymbol{n}\cdot\boldsymbol{v}} = \rho\frac{p}{\boldsymbol{n}\cdot\nabla\phi}. \tag{6}$$

This can be further written in terms of the normal derivative of the surface pressure, $\partial p/\partial n = \boldsymbol{n}\cdot\nabla p$, as

$$Z = i\omega\rho\frac{p}{\partial p/\partial n}. \tag{7}$$

Thus, the so called impedance boundary condition on the surface defines the ratio of the pressure and its normal derivative

$$\frac{\partial p}{\partial n} = i\omega\rho\frac{1}{Z}\,p. \tag{8}$$

If some parts of the surface, or the entire surface, is vibrating, the boundary condition needs to be modified according to

$$\frac{1}{\rho c Z}p + \frac{1}{ik\rho c}\frac{\partial p}{\partial n} = u_\omega, \tag{9}$$

where u_ω is the driving velocity perpendicular to the vibrating surfaces. Using definition of wavenumber k, and multiplying both sides of equation (9) with $i\omega\rho$, gives

$$\frac{ik}{Z}p + \frac{\partial p}{\partial n} = i\omega\rho u_\omega. \tag{10}$$

Writing this as

$$a\,p + b\frac{\partial p}{\partial n} = c, \tag{11}$$

with position dependent scalar functions a, b and c gives the mixed boundary condition [12] used in this work.

Boundary element formulation

Next we present the BEM formulation. Let D denote a bounded object in a homogeneous medium and S the surface of D. Assume that a time-harmonic primary acoustic wave of angular frequency ω is generated by a vibrating surface and denote the normal velocity on that surface by u_ω. Assuming no other acoustic sources the pressure of an acoustic wave p is found as a solution of homogeneous Helmholtz equation

$$\left(\nabla^2 + k^2\right) p(\boldsymbol{r}) = 0, \quad \boldsymbol{r} \in D^{\text{ext}}. \tag{12}$$

Here $\boldsymbol{r} = (x, y, z)^T$ is a point in space and D^{ext} is the background, a domain exterior to D. On surface S the pressure is assume to satisfy boundary condition (11) with given a and b and $c = i\omega\rho u_\omega$.

BEM formulation for Helmholtz equation is based on the surface integral representation that allows us to express the pressure p in terms of its Dirichlet, $p|S$, and Neumann $\partial_n p|S$, boundary values [13]

$$\Omega(\boldsymbol{r})p(\boldsymbol{r}) = \mathcal{D}[p](\boldsymbol{r}) - \mathcal{S}[\partial_n p](\boldsymbol{r}). \tag{13}$$

Here Ω is the relative solid angle subtended by the surface S. In the following, we assume that for $\boldsymbol{r} \in S$, $\Omega = 1/2$, corresponding to a (locally) smooth surface. The single and double layer surface integral operators included are defined as

$$\mathcal{S}[u](\boldsymbol{r}) = \int_S G(\boldsymbol{r}, \boldsymbol{r}') u(\boldsymbol{r}') \, dS(\boldsymbol{r}'), \tag{14}$$

$$\mathcal{D}[u](\boldsymbol{r}) = \int_S \frac{\partial G(\boldsymbol{r}, \boldsymbol{r}')}{\partial n(\boldsymbol{r}')} u(\boldsymbol{r}') \, dS(\boldsymbol{r}'), \tag{15}$$

with the fundamental solution of the Helmholtz equation in 3D, the Green's function,

$$G(\boldsymbol{r}, \boldsymbol{r}') = \frac{e^{ik|\boldsymbol{r} - \boldsymbol{r}'|}}{4\pi|\boldsymbol{r} - \boldsymbol{r}'|}. \tag{16}$$

By taking the Dirichlet and Neumann traces of (13), and combining the resulting equations with a parameter $\beta = i/k$, gives Burton-Miller integral equation [8]

$$\left(\mathcal{D} - \frac{1}{2}\mathcal{I}\right)[p] - \mathcal{S}[\partial_n p] + \beta\left(\partial_n \mathcal{D}[p] - \left(\partial_n \mathcal{S} - \frac{1}{2}\mathcal{I}\right)[\partial_n p]\right) = 0. \tag{17}$$

Here $\mathcal{I}$ is the identity operator.

Using boundary condition (11) the normal derivative of p can be expressed as

$$\partial_n p = -\frac{a}{b} p + \frac{c}{b}, \tag{18}$$

provided that $b(\boldsymbol{r}) \neq 0$ for all $\boldsymbol{r} \in S$. Substituting (18) into (17), denoting $g = c/b$ and placing all known terms to the right hand side, gives the surface integral equation to be solved

$$\left(\mathcal{D} - \frac{1}{2}\mathcal{I}\right)[p] + \mathcal{S}\left[\frac{a}{b}p\right] + \beta\left(\partial_n \mathcal{D}[p] + \left(\partial_n \mathcal{S} + \frac{1}{2}\mathcal{I}\right)\left[\frac{a}{b}p\right]\right)$$
$$= \mathcal{S}[g] + \beta\left(\partial_n \mathcal{S} + \frac{1}{2}\mathcal{I}\right)[g]. \tag{19}$$

Once the surface pressure p has been found as a solution to this equation, the sound fields outside the surface are obtained by substituting it to (13) with $\Omega = 1$ and boundary condition (18).

Weak formulation and discretization

Next a weak formulation for (19) is developed. Multiplying equation (19) with a suitable differentiable test function w in the sense of symmetric L^2 product,

$$\langle w \,,\, u \rangle = \int\limits_S w(\mathbf{r})\, u(\mathbf{r})\, dS(\mathbf{r}), \tag{20}$$

using integration by parts [8, 14], the weak formulation for (19) reads

$$\left\langle w \,,\, \left(\mathcal{D} - \frac{1}{2}\mathcal{I} \right)[p] \right\rangle + \left\langle w \,,\, \mathcal{S}\left[\frac{a}{b}p \right] \right\rangle + \beta \left(- \left\langle \mathbf{rot}\, w \,,\, \mathcal{S}(\mathbf{rot}'p) \right\rangle + k^2 \left\langle w\boldsymbol{n} \,,\, \mathcal{S}[\boldsymbol{n}'p] \right\rangle \right.$$
$$\left. + \left\langle w \,,\, \left(\partial_n \mathcal{S} + \frac{1}{2}\mathcal{I} \right)\left[\frac{a}{b}p \right] \right\rangle \right) = \left\langle w \,,\, \mathcal{S}[g] \right\rangle + \beta \left\langle w \,,\, \left(\partial_n \mathcal{S} + \frac{1}{2}\mathcal{I} \right)[g] \right\rangle. \tag{21}$$

Here $\mathbf{rot}\, w = \boldsymbol{n} \times \nabla_s u$ and $\mathbf{rot}'\, u = \boldsymbol{n}' \times \nabla_s' u$ denote the rotated surface gradient of scalar functions and $\boldsymbol{n}'$ is the normal vector at the point $\boldsymbol{r}'$. The essential feature in this form is reduction of the singularity of the operator $\partial_n \mathcal{D}$. This significantly simplifies numerical evaluation of the integrals and improves numerical stability of the solver.

Assume next that the surface of an object is divided into planar triangular elements with N nodes. By utilizing Galerkin's approach, first the unknown function p is approximated as a linear combination of basis functions $\phi_n, n = 1, \ldots, N$,

$$p(\boldsymbol{r}) \approx \sum_{n=1}^{N} c_n \phi_n(\boldsymbol{r}). \tag{22}$$

Functions $\phi_n, n = 1, \ldots, N$, are standard linear continuous nodal basis functions defined on the triangular mesh. These functions get value one at one node point of the mesh where they are defined, vanish at the other nodes, and are linear on each element.

Using functions ϕ_n as test functions, substituting approximation (22) into the weak formulation (21), leads to the matrix equation

$$\boldsymbol{A}\,\boldsymbol{x} = \boldsymbol{b}. \tag{23}$$

Here $\boldsymbol{x} = [c_1, \ldots, c_N]^T$ contains the unknowns coefficients of approximation (22). Once these coefficients are found, they are substituted to (22) to obtain an approximation of p on the surface. This approximation can be then used to find the sound pressure levels outside the surface S.

One should notice that system matrix $\boldsymbol{A}$ is dense and the matrix assembly requires evaluation of integrals with singularities. For this purpose we have developed methods based on the singularity subtraction technique [15, 10]. In these methods, two or three most singular terms are subtracted from the kernel, and computed in closed form. The remaining functions are smooth enough to allow efficient numerical integration with standard techniques. Methods to tackle problems due to the dense system matrix are introduced in the following sections.

Acceleration with multilevel fast multipole algorithm

Due to the fact that the matrix equation arising from the discretization of integral equation (19) is dense, both the memory requirement and the CPU time needed to solve the

system become prohibitive high for problems with large number of degrees of freedom (i.e. large N). Next we briefly introduce the multilevel fast multipole algorithm (MLFMA) to accelerate the calculations.

The matrix equation (23) is solved iteratively with the GMRES method. In this process one needs to be able to perform matrix-vector product with the system matrix $\boldsymbol{A}$. For this purpose the near field interactions are computed with standard BEM, resulting in a sparse matrix, and the far field interactions are computed on the fly with MLFMA for each matrix-vector product. Instead of calculating interactions of all individual sources and targets, as in standard BEM, in MLFMA the sources and targets are grouped by hierarchically dividing the object into cubes and by computing the interactions between the groups by utilizing oct-tree like data structures [16].

Traditionally MLFMA has separate algorithms for the static (low frequency) and dynamic (high frequency) cases. The high frequency version is routinely applied for problems involving objects that are significantly larger than the wavelength, but its application to complex geometries with a lot of details that are small compared to the wavelength, is much more challenging problem. The low frequency version based on multipole expansions of the field components, on the other hand, becomes inefficient at higher frequencies since the order of the required multipole expansions increases rapidly as the frequency is increased. Further, in such implementations, the out-to-in translation is not of diagonal form, which makes this operation relatively costly. The fundamental problem in MLFMA is that neither of these two versions work efficiently simultaneously in the low and high frequency regimes, or in the cases when the structure contains a lot of details that are small compared to the wavelength of an acoustic wave.

In order to enable efficient broadband simulations, or modeling of geometries requiring varying and fine element sizes, we have been working with a broadband version of MLFMA that can be applied on arbitrary mesh densities and frequencies. This algorithm is based on a hybrid multipole expansion - plane wave expansion approach. The idea is to use traditional high frequency MLFMA with Rokhlin translation function [17]

$$T(\hat{\boldsymbol{k}}, \boldsymbol{D}) = \frac{ik}{(4\pi)^2} \sum_{n=0}^{L} i^n (2n+1) \, h_n^{(1)}(k|\boldsymbol{D}|) \, P_n(\hat{\boldsymbol{D}} \cdot \hat{\boldsymbol{k}}). \tag{24}$$

for division cubes larger or equal one lambda ("super-wavelength levels"). In these levels Green's function can be represented with a plane-wave expansion

$$G(\boldsymbol{D} + \boldsymbol{d}) = \int_{S(1)} T(\hat{\boldsymbol{k}}, \boldsymbol{D}) \, e^{ik\hat{\boldsymbol{k}} \cdot \boldsymbol{d}} \, dS(\hat{\boldsymbol{k}}), \tag{25}$$

where $S(1)$ is the surface of a unit sphere, $\boldsymbol{D} = \boldsymbol{r}_c - \boldsymbol{r}_c'$ is the vector from the center of the source cube (denoted with $\boldsymbol{r}_c'$) to the center of the target cube (denoted with $\boldsymbol{r}_c$) and $\boldsymbol{d} = (\boldsymbol{r}' - \boldsymbol{r}_c') - (\boldsymbol{r} - \boldsymbol{r}_c)$. The significant benefit of (24) is that the translator is diagonal. On the other hand, the problem with (24) is that due to numerical problems it becomes unstable as the size of the cubes becomes smaller than the wavelength. As a remedy, for division cubes smaller than wavelength ("sub-wavelength levels") we utilize the low frequency stable plane wave expansion translator

$$T(\hat{\boldsymbol{k}}, \boldsymbol{D}) = \frac{ik}{8\pi^2} e^{ik\hat{\boldsymbol{k}} \cdot \boldsymbol{D}}, \qquad \boldsymbol{e}_z \cdot (\boldsymbol{D} + \boldsymbol{d}) > 0, \tag{26}$$

and the Green's function is expressed using the spectral representation

$$G(\boldsymbol{D} + \boldsymbol{d}) = \int\limits_0^{2\pi} \left(\int\limits_\Gamma T(\hat{\boldsymbol{k}}, \boldsymbol{D}) e^{ik\hat{\boldsymbol{k}}\cdot\boldsymbol{d}} \sin\theta \, d\theta \right) d\varphi. \tag{27}$$

Here the path Γ consists of two parts on the complex plane, propagating and evanescent ones [18]. The challenge is that the spectral representation is only valid in half space, and therefore requires different representations for each six main direction ($\pm x, \pm y, \pm z$). In the propagating part the direction dependency can be embedded into the translation function and exactly the same propagating representation as with the traditional Rohklin translator can be used. This makes the switch from the exponential translation function to the conventional one straightforward on the super-wavelength levels. For the evanescent part this is not possible and another approach is required. To avoid the extra aggregations/disaggregations in the evanescent part we expand the radiating and receiving field patterns for the evanescent part with multipole series. Conversion from the multipole coefficients to plane wave samples and back can then be performed quickly with the aid of fast Fourier transform (FFT) [19].

Global interpolators

The basic strategy in MLFMA is to use samples of the radiation patterns to represent outgoing fields and samples of the incoming wave patters to represent incoming fields. In order to transform samples from a level to another during the aggregation and disaggregation stages special interpolation and anterpolation routines are required, respectively [16]. This is due to the fact that the division cubes contain different amount of samples on different levels. The available interpolators can be classified as belonging to either local or global type.

Local interpolators are typically based on Lagrange interpolating polynomials [16]. They allow system matrix-vector multiplication to take place with the asymptotically favorable $O(N \log N)$ CPU-time cost, but unfortunately require oversampling of the radiation pattern. Also in practice the obtainable accuracy can be rather limited [20]. An alternative for local interpolators is the global interpolator based on trigonometric polynomial expansions [21, 6]. Such presentations have several useful properties: Conversion between sample values and coefficients of the expansion can be performed effectively and accurately with FFT. Global interpolators allow the storage of the sampled radiation pattern components to take place in significantly reduced size compared to other alternatives, and are used in this work.

Efficient evaluation of the source term

In cases where the source of an acoustics wave is generated by a vibrating surface, and that surface is very large, e.g., the entire structure, the computation of an acoustic source, the right hand side of (19), becomes a very expensive task. The computations scale similarly as the assembly of the original matrix equation. To avoid that, we have applied MLFMA to accelerate evaluation of the source term. This significantly improves the speed of the algorithm in cases where large vibrating surfaces are present.
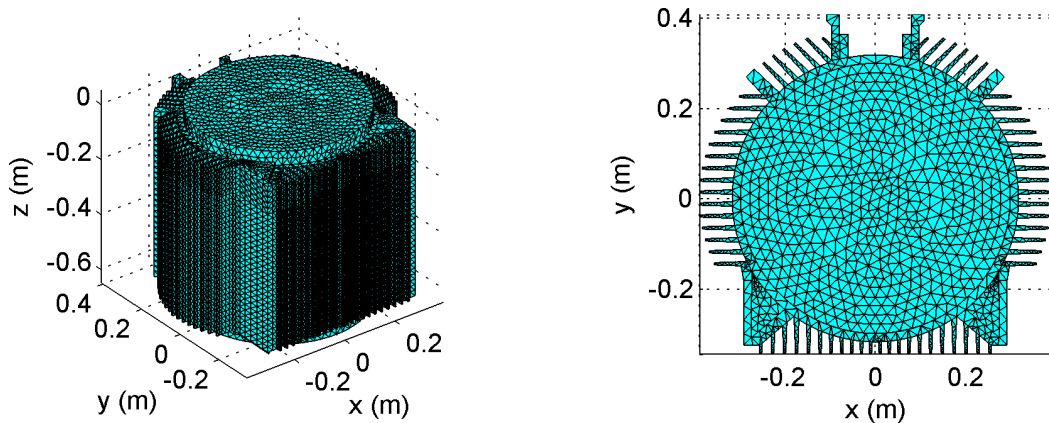
Figure 1. The geometry of an electric motor. The surface mesh consists of 54984 triangular elements and 27494 nodes.

Simulation examples

As a model problem we investigate sound emission from an electric motor. The used motor structure is simplified, typical 2-pole, 200 kW rib-cooled squirrel-cage induction motor. The model geometry is shown in Fig. 1. The aim is to imitate the standardized measurement approach (ISO-3745 [22]) to obtain the radiated sound power for the motor at a given excitation. The measurement standard uses 20 equidistantly arranged microphones in an anechoic space or 10 microphones in hemi-anechoic conditions. The sound power is obtained by integrating pressure measurement data from all microphones. Since the simulations can be easily extended to a large number of "virtual microphones", we shall show how the changes in the number of measurement points affects the sound power results.

We focus on the frequency range from 10 to 3410 Hz which is simulated in 100 Hz steps. Two methods are compared for the sound power computations. First, the high-frequency boundary element method (HFBEM) [23], is a Rayleigh integral type method which assumes ray-like sound propagation and neglects many physical sound phenomena such as diffraction and scattering. HFBEM is, however, relatively accurate for sound power simulations and commonly used due to its simplicity. Second method, which is referred as the fast boundary element method (FBEM), is outlined in the previous sections of this study. FBEM is a full-wave method and the solution includes all physical phenomena characterized by the acoustic wave equation.

In both cases, the simulation work has the following steps:

1. The motor structure is modeled with FEM using Comsol Multiphysics.

2. Computation of complex eigenmodes up to 5 kHz is then carried out using material model with hysteretic damping. Isotropic steel material properties with constant structural loss factor of 1 % for casing and 0.5 % for stator (complex Young's modulus) were used in the FEM-simulations.

3. The modes are then imported to MATLAB for unit-wave response computation using modal superposition and. Rotating radial unit-force wave applied on stator surface (teeth) $F_r = \exp\left(i(r\phi - wt)\right)\mathbf{u}_r$ in cylindrical coordinates with $r = 4$. The FEM based unit-wave responses for an electric motor are discussed in more detail in [24].
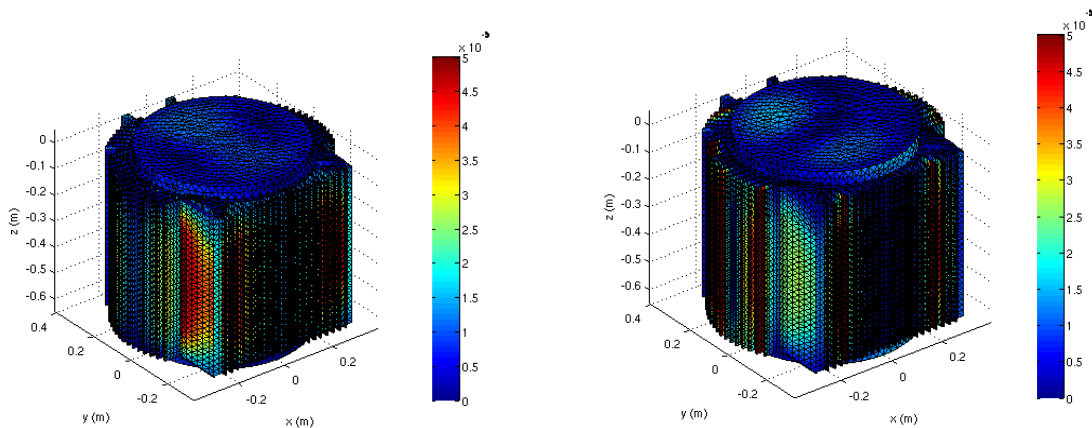
Figure 2. The normal surface velocity magnitude at two frequencies: 1110 Hz (left) and 1910 Hz (right).

4. The surface velocities for each frequency are extracted from the structural dynamic simulations. The complex valued velocity is constant for each surface triangle of the BE mesh. The BE mesh, consisting of 54984 surface elements and 27494 nodes, is shown in Fig. 1. We note that the number of nodes is also the number of degrees of freedom of the BE model.

5. The normal velocity of the surface is given as the boundary condition to the BE model. We assume that the surface is rigid and set $a = 0$ and $b = 1$ in Eq. (11).

6. In FBEM, the acoustic pressure on the surface is solved from (19) for given normal velocity distribution. To evaluate the sound pressure levels outside the surface, the solution on the surface is substituted to (13) with $\Omega = 0, a = 0$ and $b = 1$.

Two normal surface velocity distributions that are extracted from the FEM computations are shown in Fig. 2. The frequencies are chosen to correspond the peak value of the radiated power (at 1110 Hz) and the frequency on which the FBEM and HFBEM methods have a large disagreement (1910 Hz, see Fig. 6).

The locations of the measurement points (virtual microphones) are shown in Fig. 3. Opposed to the ISO measurement standard, which uses 20 microphones in an anechoic case, the number of virtual microphones ranges from 812 to 15095. The effect of the measurement point density can be seen from Figs. 4 and 5. For both methods, the coarse point set gives a visible disagreement with the two dense point sets when the frequency exceeds 1500 Hz. The discrepancy is 3-4dB at the highest frequencies. On the other hand, the dense and extra dense point sets give a good agreement over the entire frequency range.

In Fig. 6, HFBEM and FBEM results are compared using the dense set of measurement points. The largest disagreement can be observed at the lowest frequencies and in the range 1500-2000 Hz.

Conclusions

In this study, a fast boundary element method (FBEM) is introduced for simulating acoustic emission from a vibrating structure. An electric motor is used as a model problem. FBEM is based on the full-wave acoustic BE model accelerated with multilevel fast multipole algorithm (MLFMA). A special version of MLFMA is introduced. This algorithm allows efficient and accurate acoustic modeling of large structures with fine details on a
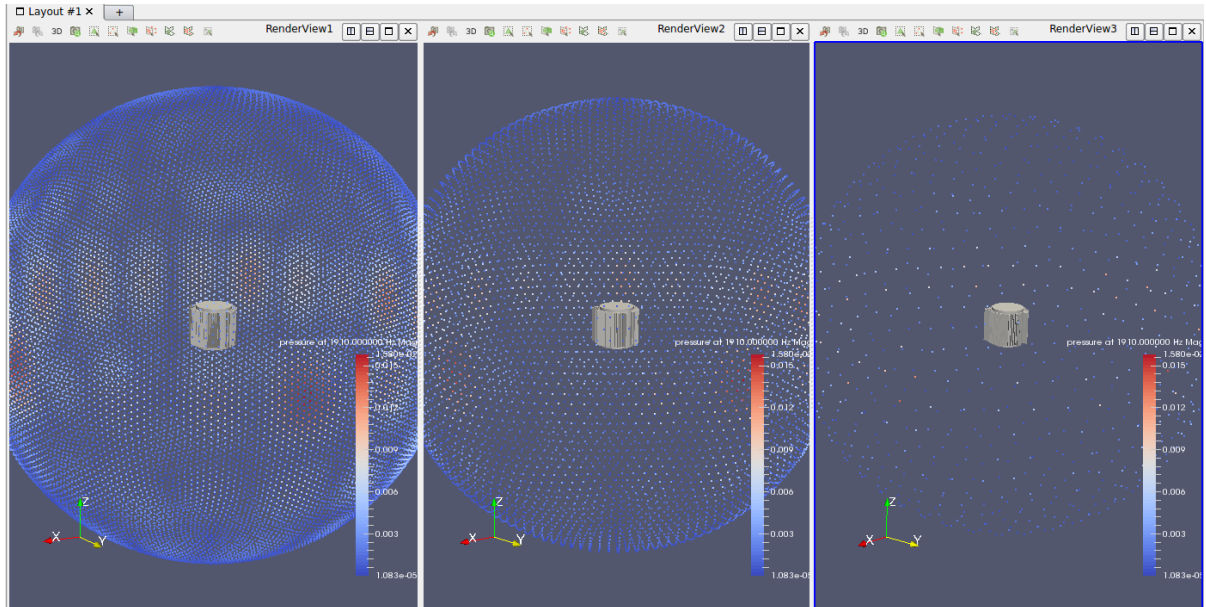
Figure 3. The virtual microphone locations used in the simulations. The *extra dense* set consists of 15095 measurement points (left), the *dense* has 7292 points (middle) and the *coarse* set has 812 virtual microphone locations (right). The motor is positioned at the center of the measurement points.
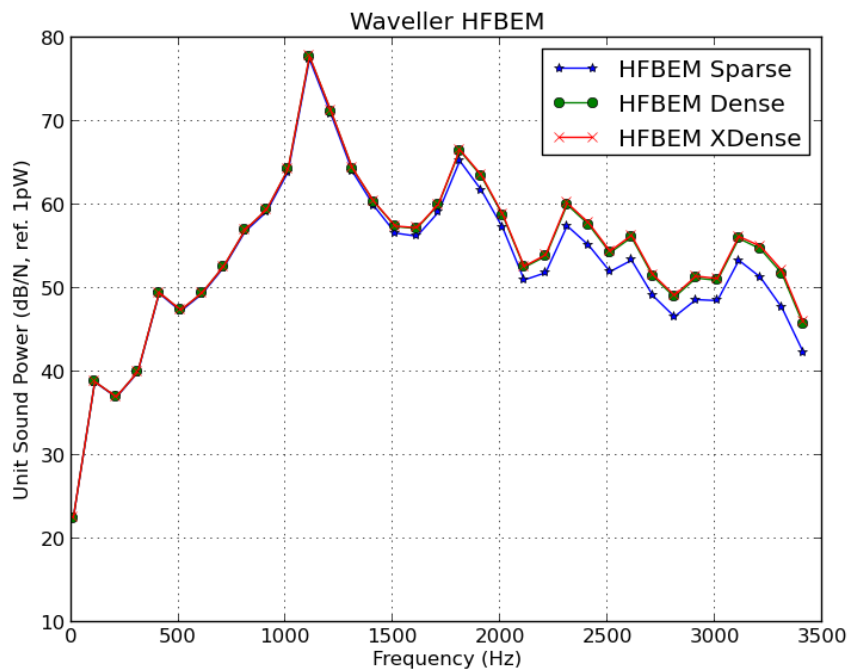
Figure 4. The comparison of radiated sound power levels using HFBEM and a different number of measurement points.
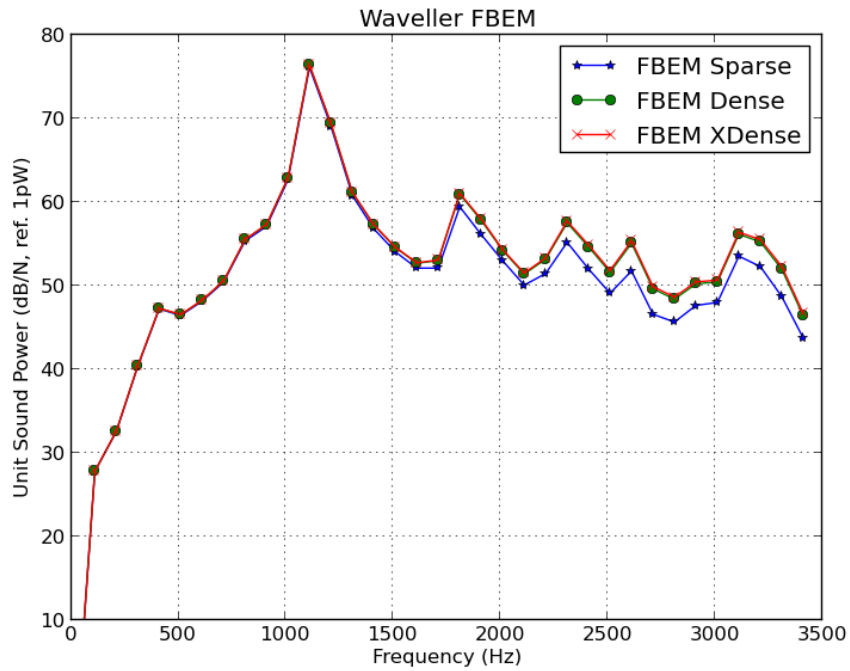
Figure 5. The comparison of radiated sound power levels using FBEM and a different number of measurement points.
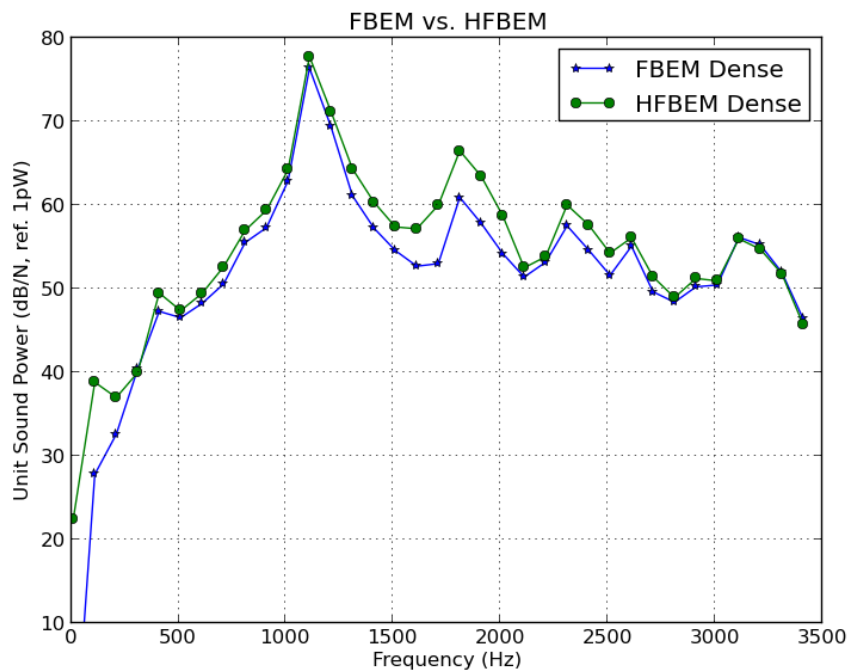
Figure 6. The comparison of the radiated sound power levels that are computed using HFBEM and FBEM; and the "dense" set of measurement points.

broad range of frequencies. The surface velocity distribution of the structure, computed using a finite element method (FEM), is used as a source in acoustic FBEM.

A comparison of FBEM with a simplified sound propagation model (HFBEM) reveals notable disagreement at low frequencies (>10dB), but, more importantly, also at frequencies 1500-2000Hz which provide more significant contribution on the A-weighted decibel scale. While the detailed analysis of the discrepancies is a topic of our next study, it can be hypothesized that lower sound powers obtained using the FBEM are associated with the finned structure of electric motor. Possibly, acoustic resonances in the air space between fins (which are not taken into account by HFBEM) affect the overall radiation of the sound.

The second interesting observation was that to model the radiated sound power accurately, the number of measurement points surrounding the structure need to be large enough. Especially at higher frequencies, sound may "leak" between measurement points resulting to erroneous sound power estimates.

Acknowledgement

References

[1] R.D. Ciskowski, C.A Brebbia (Editors), *Boundary Element Methods in Acoustics*, Computational Mechanics Publications, Southampton, 1991.

[2] S. Kirkup, *The Boundary Element Method in Acoustics*, 2007. doi:10.1016/S0218-396X(00)00016-9.

[3] N.A. Gumerov and R. Duraiswami, *Fast multipole methods for the Helmholtz equation in three dimensions*, Elevier, 2004.

[4] Y. Liu, L. Shen, and M. Bapat, Development of the fast multipole boundary element method for acoustic wave problems, *Recent Advances in Boundary Element Methods*, Springer, 287–303,2009.

[5] H. Wallén, S. Järvenpää, and P. Ylä-Oijala, Broadband multilevel fast multipole algorithm for acoustic scattering problems, *Journal of Computational Acoustics*, 14(4):507–526,2006. doi:10.1142/S0218396X06003153.

[6] S. Järvenpää, and P. Ylä-Oijala, Multilevel fast multipole algorithm with global and local interpolators, *IEEE Transactions on Antennas and Propagation*, 62(9):4716–4725,2014. doi:10.1109/TAP.2014.2333056.

[7] S. Järvenpää, and P. Ylä-Oijala, A global interpolator with low sample rate for multilevel fast multipole algorithm, *IEEE Transactions on Antennas and Propagation*, 61(3),1291–1300,2013. doi:10.1109/TAP.2012.2231927.

[8] A.J. Burton and G.F. Miller, The application of integral equation methods to numerical solutions of some exterior boundary value problem, *Proceedings of the Royal Society London Ser A*, 323:210–210,1971.

[9] P. Ylä-Oijala and S. Järvenpää, Iterative solution of high-order boundary element method for acoustic impedance boundary value problems, *Journal of Sound and Vibration*, 291:824–843,2006. doi:10.1016/j.jsv.2005.06.044.

[10] S. Järvenpää, M. Taskinen, and P. Ylä-Oijala, Singularity subtraction technique for high-order polynomial vector basis functions on planar triangles, *IEEE Transactions on Antennas and Propagation*, 54(1):42–49,2006. doi:10.1109/TAP.2005.861556.

[11] P. Ylä-Oijala, S.P. Kiminki, and S. Järvenpää, Conforming boundary element methods in acoustics, *Engineering Analysis with Boundary Elements*, 50:447–458,2015. doi:10.1016/j.enganabound.2014.10.002.

[12] N.A. Gumerov and R. Duraiswami, A broadband fast multipole accelerated boundary element method for the three dimensional Helmholtz equation, *Journal of Acoustical Society of America*, 125(1):191–205,2009. doi:10.1121/1.3021297.

[13] D. Colton and R. Kress, *Integral Equation Methods in Scattering Theory*, John Wiley & Sons, New York, 1983.

[14] L. Demkowicz, A. Karafiat, and J. T. Oden, Variational (weak) form of the hypersingular formulation for the Helmholtz exterior boundary-value problems, *TICOM Report 91-05, The Texas institute for Computational Mechanics*, 1991.

[15] S. Järvenpää, M. Taskinen, and P. Ylä-Oijala, Singularity extraction technique for integral equation methods with high order basis functions on plane triangles and tetrahedra, *International Journal for Numerical Methods in Engineering*, 58:1149–1165,2003. doi:10.1002/nme.810.

[16] W.C. Chew, J.-M. Jin, E. Michielssen, and J. Song, *Fast and Efficient Algorithms in Computational Electromagnetics*, Artech House, Boston, 2001.

[17] V. Rokhlin, Rapid solution of integral equations of scattering theory in two dimensions, *Journal of Computational Physics*, 86(2),414–439,1990. doi:10.1016/0021-9991(90)90107-C.

[18] H. Wallén and J. Sarvas, Translation procedures for broadband MLFMA, *Progress in Electromagnetic Research*, 55:47–78,2005. doi:10.2528/PIER05021001.

[19] S. Järvenpää and H. Wallén, Improvements to the numerical computation of the evanecent part in broadband MLFMA, *2015 IEEE International Symposium on Antennas and Propagation and North American Radio Science Meeting*, 19-25 July 2015, Vancouver, BC,Canada. doi:10.1109/USNC-URSI.2015.7303369.

[20] S. Koc, J. Song, and W.C. Chew, Error analysis for the numerical evaluation of the diagonal forms of the scalar spherical addition theorem, *SIAM Journal of Numerical Analysis*, 36(3),906–921,1999. doi:10.1137/S0036142997328111.

[21] J. Sarvas, Performing interpolation and anterpolation entirely by fast Fourier transform in the 3D multilevel fast multipole algorithm, *SIAM Journal of Numerical Analysis*, 41(6):2180–2196,2003. doi:10.1137/S0036142902405655.

[22] ISO 3745:2003, Acoustics - Determination of sound power levels of noise sources using sound pressure - Precision methods for anechoic and hemi-anechoic rooms, 2003.

[23] D.W. Herrin, F. Martinus, T.W. Wu, and A.F. Seybert, A new look at the high frequency boundary element and Rayleigh integral approximations, *SAE Technical Paper*, 2003.

[24] J. Roivainen, Unit-wave response-based modeling of electromechanical noise and vibration of electrical machines, PhD Thesis, Helsinki University of Technology, 2009.

Pasi Ylä-Oijala, Seppo Järvenpää
Department of Radio Science and Engineering, Aalto University
P.O. Box 3000, FI-00076 AALTO
`pasi.yla-oijala@aalto.fi, seppo.jarvenpaa@aalto.fi`

Tomi Huttunen, Antti Vanne, Matti Malinen
Kuava Ltd.
Microkatu 1, FI-70210 Kuopio, Finland
`tomi.huttunen@kuava.fi`

Janne Roivainen
ABB Motors and Generators
`janne.roivainen@fi.abb.com`